Program Digest, 2019 IEEE International Ultrasonics Symposium (IUS)
Glasgow, Scotland, October 6-9, 2019

In vitro Preparation and Characterization of Magnetic Nanobubbles

Xiaolei Yi
Department of Ultrasound Shanghai Jiaotong University Affiliated Sixth People's Hospital
Shanghai, China
yixiaolei1982@163.com

Eric C. Abenojar
Department of Radiology Case Western Reserve University
Cleveland, OH, USA
eric.abenojar@case.edu

Jinle Zhu
Department of Radiology Case Western Reserve University
Cleveland, OH, USA
jinle.zhu@case.eu

Yuanyi Zheng
Department of Ultrasound Shanghai Jiaotong University Affiliated Sixth People's Hospital
Shanghai, China
zhengyuanyi@163.com

Agata A. Exner
Department of Radiology Case Western Reserve University
Cleveland, OH, USA
agata.exner@case.edu

***Abstract*—Lipid-shelled magnetic bubbles are widely researched for potential applications as multi-functional contrast agents for ultrasound and magnetic resonance imaging and for drug delivery applications. In this study, we prepared nano-sized magnetic bubbles using a magnetic lipid solution created by first forming a homogeneous phospholipid solution in phosphate buffered saline (PBS) containing glycerol and propylene glycol and followed by adding superparamagnetic iron oxide nanoparticles with a diameter of 10 nm. Bubbles were generated by mechanical agitation using a dental amalgamator, and magnetic nanobubbles were isolated by centrifugation at 50 *g* for 5 min. Prepared magnetic nanobubbles had a mean diameter of 308 ± 105 nm and a concentration of (1.68 x 10^{10} bubbles/mL), as determined by resonant mass measurement. Stability of the magnetic nanobubbles over time was evaluated by measuring the acoustic signal decay. Magnetic nanobubbles showed a 27% and 83% signal decay after 1 and 2 h at room temperature, respectively. The response of the magnetic nanobubbles to a magnetic field was examined by measuring T_2 relaxation times at different bubble/iron concentrations. Magnetic nanobubbles showed an r_2 relaxivity of 144.6 $mM^{-1}s^{-1}$. This study demonstrates feasibility of preparing magnetic nanobubbles using a simple self-assembly process. The constructs could be more effective in multimodality molecular imaging and extravascular drug delivery compared to magnetic microbubbles, due to their sub-micron size.**

Keywords—Ultrasound Contrast Agents, Magnetic Nanobubbles, Resonant Mass Measurement

I. INTRODUCTION

Ultrasound is widely used in clinical diagnostic imaging because it is inexpensive, safe, and portable. Much recent research has focused on the use of perfluorocarbon core, lipid-shelled bubbles as echogenic contrast agents to improve ultrasound imaging contrast resolution by enhancing backscatter echo signal due to acoustic impedance mismatch between the gas in the bubbles and the surrounding tissue [1]. Bubble shell chemistry can be exploited to expand bubble functionality, adding molecular targeting [2], drug delivery [3], and multi-modality imaging capabilities [4]. For instance, addition of magnetic nanoparticles to the shell allows for dual modality contrast generation using ultrasound and magnetic resonance imaging (MRI) [5]. Further, magnetically guided drug delivery can be also explored with this system, thus creating a convenient theranostic agent providing simultaneous therapeutic and diagnostic benefits [6]. Iron oxide nanoparticles are typically used as the magnetic component in bubbles because they are relatively low cost, generally safe, and highly biocompatible [7].

Different strategies to incorporate magnetic components into microbubbles have been reported. These are classified based on the location of the magnetic particles within the bubble: (a) inside the bubble, (b) embedded in the bubble shell, and (c) conjugated to the bubble surface [8]. While significant effort has been devoted to the preparation of micron-sized magnetic bubbles [8]–[10], fewer reports are available regarding magnetic lipid-shelled nanobubble preparation. Polymers such as polyacrylic acid (PAA), poly(lactic-co-glycolic acid), and polystyrene have been used as the shell material embedded with magnetic nanoparticles to prepare magnetic nanobubbles [11]–[13]. Phospholipid-based magnetic nanobubbles have been reported for drug delivery applications [14]. In this case, the thin film hydration technique was used to prepare a lipid solution followed by addition of water-soluble magnetic nanoparticles conjugated with a drug. The magnetic nanoparticles were prepared using the co-precipitation method [14].

The objective of this work was to provide an alternative method to prepare magnetic nanobubble samples using hydrophobic iron oxide magnetic nanoparticles. Here, we report on a simple self-assembly method to prepare lipid shell-stabilized perfluoropropane (C_3F_8) magnetic nanobubbles by

embedding 10 nm monodisperse hydrophobic iron oxide nanoparticles in the nanobubble shell. The prepared samples were further characterized for potential use in ultrasound and MRI applications by *in vitro* ultrasound and T_2 relaxivity measurements.

II. Methods and Experimental Section

A. Materials

The lipids DBPC (1,2-dibehenoyl-sn-glycero-3-phosphocholine), and 1,2-dipalmitoyl-sn-glycero-3-phosphate (DPPA) were purchased from Avanti Polar Lipids (Pelham, AL, USA). 1,2- dipalmitoyl-sn-glycero-3-phosphoethanolamine (DPPE) was obtained from Corden Pharma (Switzerland), and mPEG-DSPE (1,2-distearoyl-*sn*-glycero-3-phosphoethanolamine-N-[methoxy(polyethylene glycol)-2000] (ammonium salt)) was obtained from Laysan Lipids (Arab, AL, USA). Glycerol (99+%, Acros Organics) and phosphate buffered saline solution (PBS, Gibco, Life Technologies) were purchased from Fisher Scientific (Pittsburgh, PA, USA). Propylene glycol was purchased from Sigma Aldrich (Milwaukee, WI, USA). Perfluoropropane (C_3F_8) was obtained from AirGas (Cleveland, OH, USA). Oleic acid-coated iron oxide nanoparticles (10 nm) were purchased from Ocean Nanotech (San Diego, USA).

B. Magnetic Nanobubble Formulation

Magnetic, lipid shell-stabilized bubbles were prepared using a combination of lipids (DBPC, DPPE, DPPA, mPEG-DSPE) dissolved in a mixture of propylene glycol and glycerol in phosphate buffered saline (PBS). Oleic acid-coated iron nanoparticles (Fe_3O_4) were then added to the lipid solution and sonicated until a homogeneous solution was obtained. Following gas exchange, iron oxide-lipid solutions were activated using a Vialmix dental amalgamator (Bristol- Myers Squibb Medical Imaging, Inc., N. Billerica, MA, USA) for 45 s to generate polydisperse bubbles. Magnetic nanobubbles were then isolated via centrifugation at 50 *g* for 5 min. Plain nanobubbles were prepared in a similar fashion as above but without the addition of magnetic nanoparticles [15].

C. Size and Concentration Characterization

Bubble size and concentration were characterized using resonant mass measurement (RMM) (Archimedes, Malvern Panalytical Inc., Westborough, MA) which measures particle mean diameter, size distribution, and concentration using a nanosensor [16]. The sensor and microfluidic tubing were cleaned with deionized water between each run. Data was exported from the Archimedes software (version 1.2). Measurements were made at different time points (t = 0, 0.5, 1, 1.5, and 2 h) by preparing magnetic nanobubbles at 1:100 dilution and plain nanobubbles at 1:1000 dilution and storing at room temperature prior to measurement.

D. Transmission Electron Microscopy Imaging

Magnetic nanobubble morphology was imaged via transmission electron microscopy (TEM) using a previously reported method in literature [17]. Samples were prepared for imaging by placing 10 µL of a dilute suspension of the samples on a 400 mesh Formvar-coated copper grid upside down for 1 min. The sample was then stained by placing it on top of a 20 µL droplet of 2% uranyl acetate for 30 s and the excess was removed. The TEM grid containing the bubble sample was allowed to dry for another 30 min. TEM images were obtained with a FEI Tecnai G2 Spirit BioTWIN transmission electron microscope operated at 120 kV.

E. Characterization of Acoustic Activity and Bubble Stability

The acoustic activity and stability of magnetic NBs in solution was evaluated using a clinical ultrasound (Toshiba Aplio XG, SSA-790A, Toshiba Medical Imaging Systems, Otawara-Shi, Japan) equipped with a PLT-1204BT linear transducer. Bubbles were placed in 1.5% (w/v) agarose phantom molds containing three channels (L x W x H = 5 x 3 x 6 mm). Ultrasound measurements were made at different time points (t = 0, 0.5, 1, 1.5, and 2 h) by preparing magnetic nanobubbles at 1:100 dilution and storing at room temperature prior to measurement. Ultrasound parameters were set to contrast harmonic imaging (CHI) with 12.0 MHz harmonic frequency, 0.10 mechanical index (MI), 65 dB dynamic range, and 70 dB gain. The signal for each time point was analyzed using the onboard quantification software (CHI-Q). The mean signal intensity per region of interest (ROI) was drawn for each image and initial signal enhancement was quantified using exported data and analyzed by subtracting background signal [18].

F. T_2 Relaxivity Measurements

The T_2 relaxivity of the magnetic nanobubbles were measured using a 1.5 T 60 MHz Bruker Minispec NMR relaxometer. R_2 relaxivity value was determined by measuring T_2 relaxation times of the bubbles diluted in PBS at different iron (Fe) concentrations and using the following equation:

$$\frac{1}{T_{2(sample)}} = \frac{1}{T_{2(solvent)}} + r_2[M] \qquad (1)$$

The Fe concentration in magnetic bubbles was determined via atomic absorption spectroscopy (AAS). The samples were placed in concentrated hydrochloric acid solution (HCl, 37%) to fully digest the samples and diluted with Millipore deionized water prior to measurement. Fe concentration in the samples was quantified using a calibration curve composed of 0, 1, 5, 10, 15, and 25 ppm Fe AAS standard solutions.

III. Results and Discussion

The magnetic nanobubble samples were prepared by making a homogeneous magnetic lipid solution consisting of lipids (DBPC, DPPA, DPPE, and mPEG-DSPE) and a magnetic nanoparticle 10 nm in diameter in a PBS matrix containing propylene glycol and glycerol. The size and concentration of magnetic nanobubbles were measured with Archimedes RMM and compared to plain nanobubbles for reference. Fig. 1 (a) and (c) show the size of magnetic and plain nanobubbles, respectively. Magnetic and plain nanobubbles showed comparable mean diameters of 308 ± 105 nm and 283 ± 109 nm, respectively. Samples diluted and left at room temperature after 0.5 to 2 h showed a reduction in size that was comparable for both bubble types: magnetic nanobubbles ranged from 201 nm to 215 nm and plain

nanobubbles ranged from 188 nm to 199 nm, which corresponds to a decrease in size of 30.2%–34.7% and 29.7%–33.6%, respectively. Bubble sizes were comparable for both samples from 0.5–2 h most likely because the bubbles reached a quasi-static equilibrium in terms of its size and with the concentration of the gas in the bubble and the surrounding matrix [16]. The sudden decrease in size that occurred after 0. 5 h is likely due to exposure of the bubbles to higher (room) temperature leading to bubble dissolution or slow diffusion of gas out the bubbles. Because the samples were diluted and left at room temperature during the waiting time period prior to measurement, gas diffusion out of the bubbles was enhanced due to the increase in concentration gradient difference between the gas and the PBS solvent. A similar trend was observed for the concentration of bubbles over time as seen in Fig. 1 (b) and (d). The mean bubble concentration of magnetic nanobubbles was 1.68×10^{10} bubbles/mL, compared to 2.64×10^{11} bubbles/mL for plain nanobubbles. The addition of magnetic particles led to over a ten-fold decrease in bubbles produced suggesting that magnetic nanoparticles interfered with the production of stable bubbles. Likewise, the concentration decreased rapidly after 0.5 h but was comparable from 0.5 h to 2 h, which can be explained similar to that of the trends observed for size variation over time.

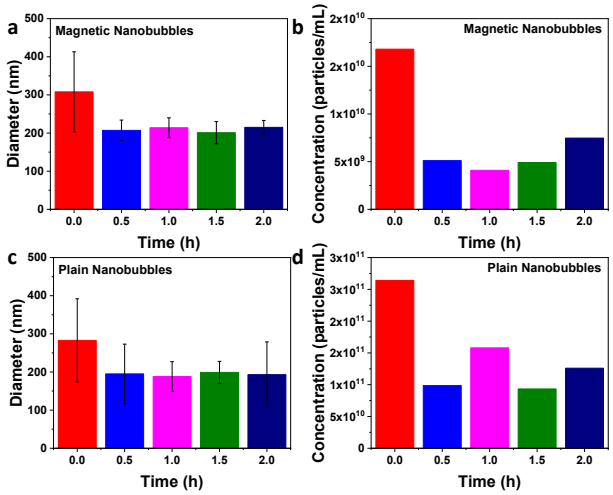

Fig. 1. (a) and (b) The size and concentration of magnetic nanobubbles, (c) and (d) the size and concentration of plain nanobubbles.

In vitro ultrasound measurements of magnetic nanobubbles over time from 0–2 h are shown in Fig. 2. A progressive decrease in ultrasound signal enhancement was observed (27% and 83% after 1 and 2 h, respectively, Fig. 2 (a)). This can also be seen in the corresponding nonlinear contrast mode images observed in Fig. 2 (b). The signal enhancement decay over time for the magnetic nanobubbles is more rapid compared to plain nanobubbles that were analyzed in the same way in a previously published report [16]. This could most likely be due to the instability brought about by the addition of the magnetic nanoparticles into the bubble shell. In addition, size and concentration were comparable from 0.5–2 h time points but progressively decreased under ultrasound exposure indicating that the acoustic activity measurement is more sensitive to detect changes in bubble stability and concentration over time [1].

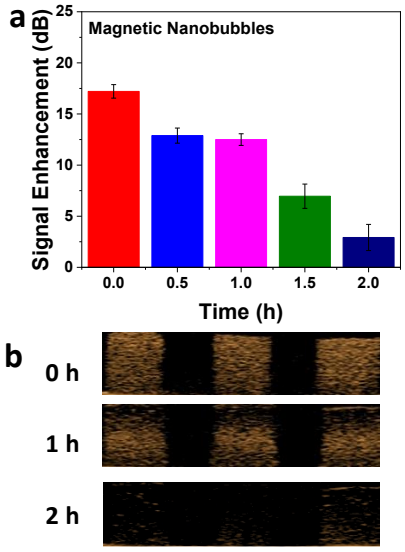

Fig. 2. *In vitro* ultrasound stability characterization: (a) changes in signal enhancement (dB) of magnetic nanobubbles over time, and (b) corresponding nonlinear contrast mode ultrasound images at the indicated time points.

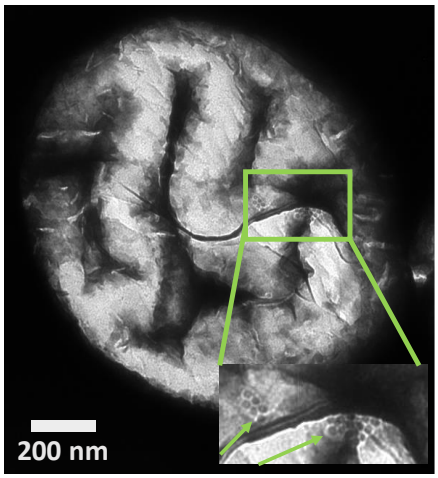

Fig. 3. Representative TEM image of a magnetic nanobubble. Inset picture shows the magnetic nanoparticles (green arrow) in the bubble.

Magnetic nanobubbles were also visualized using TEM (Fig. 3). Electron microscopy images confirmed the presence of magnetic nanoparticles in the bubble. Bubble morphology was similar to that previously reported literature, with bubbles shown as circular objects and some discontinuities corresponding to folds in the phospholipid shell [17].

The MRI performance of the magnetic nanobubbles was also evaluated by measuring the T_2 relaxation rates of the samples at different Fe concentrations using a 1.5 T 60 MHz Bruker Minispec NMR relaxometer (Fig. 4). T_2 relaxation rates increased with increasing Fe concentration due to higher sample magnetization. r_2 relaxivities were quantified based on equation (1) generated from the equation of the line in the T_2 relaxation rate vs. Fe concentration plot. Magnetic nanobubbles

showed an r_2 relaxivity (144.6 $mM^{-1} \cdot s^{-1}$) that is almost 47% higher than the reported value for commercially available iron oxide MRI contrast agent Resovist (Table 1) [5]. This indicates that it has good potential for MRI imaging applications *in vivo*.

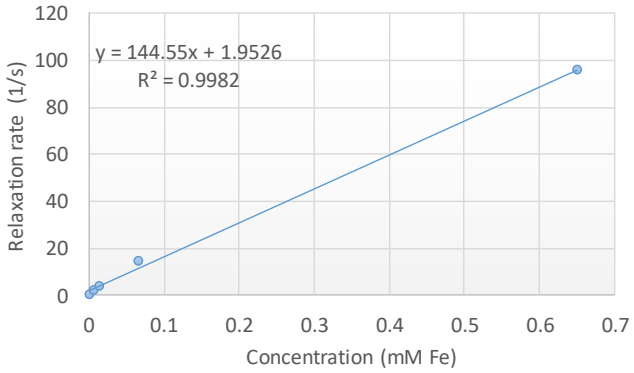

Fig. 4. T_2 relaxation rate vs. Fe concentration of magnetic nanobubbles.

TABLE I. R_2 relaxivity of magnetic bubble samples

Sample	r_2 relaxivity ($mM^{-1}s^{-1}$)
Magnetic nanobubbles	144.6
Resovist [5]	98.4

IV. Conclusion

In summary, we have prepared iron oxide-loaded nanobubbles with a size of 308 ± 105 nm with robust acoustic and magnetic properties suitable for potential ultrasound and MRI contrast imaging. We plan to perform future studies examining the *in vivo* ultrasound and MRI performance of these constructs.

Acknowledgment

This work was supported in part by the National Institute of Biomedical Imaging and Bioengineering (NIBIB) of the NIH under Award No. R01-EB025741. The content is solely the responsibility of the authors and does not necessarily represent the official views of the National Institutes of Health and National Institute of Biomedical Imaging and Bioengineering. For X.Y., this work was supported in part by the Youth Science Fund Project of National Natural Science Foundation of China (NSFC) under Award No.81701700 and NSFC Key Projects of International Cooperation and Exchanges (under Award No.81720108023).

References

[1] E. C. Abenojar *et al.*, "Effect of Bubble Concentration on the in Vitro and in Vivo Performance of Highly Stable Lipid Shell-Stabilized Micro- and Nanoscale Ultrasound Contrast Agents," *Langmuir*, vol. 35, no. 31, pp. 10192–10202, Aug. 2019.

[2] Y. Gao *et al.*, "Ultrasound molecular imaging of ovarian cancer with CA-125 targeted nanobubble contrast agents," *Nanomedicine Nanotechnology, Biol. Med.*, vol. 13, no. 7, pp. 2159–2168, Oct. 2017.

[3] R. Cavalli, M. Soster, and M. Argenziano, "Nanobubbles: a promising efficienft tool for therapeutic delivery," *Ther. Deliv.*, vol. 7, no. 2, pp. 117–138, Feb. 2016.

[4] J. E. Lemaster, F. Chen, T. Kim, A. Hariri, and J. V. Jokerst, "Development of a Trimodal Contrast Agent for Acoustic and Magnetic Particle Imaging of Stem Cells," *ACS Appl. Nano Mater.*, vol. 1, no. 3, pp. 1321–1331, Mar. 2018.

[5] C.-H. Fan *et al.*, "SPIO-conjugated, doxorubicin-loaded microbubbles for concurrent MRI and focused-ultrasound enhanced brain-tumor drug delivery," *Biomaterials*, vol. 34, no. 14, pp. 3706–3715, May 2013.

[6] C. A. Sennoga *et al.*, "Microbubble-mediated ultrasound drug-delivery and therapeutic monitoring," *Expert Opin. Drug Deliv.*, vol. 14, no. 9, pp. 1031–1043, Sep. 2017.

[7] S. Laurent *et al.*, "Magnetic Iron Oxide Nanoparticles: Synthesis, Stabilization, Vectorization, Physicochemical Characterizations, and Biological Applications," *Chem. Rev.*, vol. 108, no. 6, pp. 2064–2110, Jun. 2008.

[8] E. Beguin, L. Bau, S. Shrivastava, and E. Stride, "Comparing Strategies for Magnetic Functionalization of Microbubbles," *ACS Appl. Mater. Interfaces*, vol. 11, no. 2, pp. 1829–1840, Jan. 2019.

[9] T. B. Brismar *et al.*, "Magnetite Nanoparticles Can Be Coupled to Microbubbles to Support Multimodal Imaging," *Biomacromolecules*, vol. 13, no. 5, pp. 1390–1399, May 2012.

[10] X. Cai, F. Yang, and N. Gu, "Applications of Magnetic Microbubbles for Theranostics," *Theranostics*, vol. 2, no. 1, pp. 103–112, 2012.

[11] H.-Y. Huang *et al.*, "A Multitheragnostic Nanobubble System to Induce Blood-Brain Barrier Disruption with Magnetically Guided Focused Ultrasound," *Adv. Mater.*, vol. 27, no. 4, pp. 655–661, Jan. 2015.

[12] W. Song *et al.*, "Magnetic nanobubbles with potential for targeted drug delivery and trimodal imaging in breast cancer: an *in vitro* study," *Nanomedicine*, vol. 12, no. 9, pp. 991–1009, May 2017.

[13] H.-Y. Huang *et al.*, "SPIO nanoparticle-stabilized PAA-F127 thermosensitive nanobubbles with MR/US dual-modality imaging and HIFU-triggered drug release for magnetically guided in vivo tumor therapy," *J. Control. Release*, vol. 172, no. 1, pp. 118–127, Nov. 2013.

[14] Ş. Hamarat Şanlıer *et al.*, "Development of Ultrasound-Triggered and Magnetic-Targeted Nanobubble System for Dual-Drug Delivery," *J. Pharm. Sci.*, vol. 108, no. 3, pp. 1272–1283, Mar. 2019.

[15] A. de Leon *et al.*, "Contrast enhanced ultrasound imaging by nature-inspired ultrastable echogenic nanobubbles," *Nanoscale*, vol. 11, no. 33, pp. 15647–15658, Aug. 2019.

[16] C. Hernandez *et al.*, "Sink or float? Characterization of shell-stabilized bulk nanobubbles using a resonant mass measurement technique," *Nanoscale*, vol. 11, no. 3, pp. 851–855, Jan. 2019.

[17] J. Owen and E. Stride, "Technique for the Characterization of Phospholipid Microbubbles Coatings by Transmission Electron Microscopy," *Ultrasound Med. Biol.*, vol. 41, no. 12, pp. 3253–3258, Dec. 2015.

[18] C. Hernandez, L. Nieves, A. C. de Leon, R. Advincula, and A. A. Exner, "Role of Surface Tension in Gas Nanobubble Stability Under Ultrasound," *ACS Appl. Mater. Interfaces*, vol. 10, no. 12, pp. 9949–9956, Mar. 2018.